



<b>Publication Year</b>	2009
<b>Acceptance in OA@INAF</b>	2023-01-24T11:35:30Z
<b>Title</b>	þý A G I L E detection of a rapid <sup>3</sup> -ray flare from the blazar GASP-WEBT monitoring
<b>Authors</b>	D'AMMANDO, FILIPPO; Pucella, G.; RAITERI, Claudia Maria; VILLATA, Massimo; VITTORINI, VALERIO; et al.
<b>DOI</b>	10.1051/0004-6361/200912560
<b>Handle</b>	<a href="http://hdl.handle.net/20.500.12386/33026">http://hdl.handle.net/20.500.12386/33026</a>
<b>Journal</b>	ASTRONOMY & ASTROPHYSICS
<b>Number</b>	508

# AGILE detection of a rapid $\gamma$ -ray flare from the blazar PKS 1510-089 during the GASP-WEBT monitoring<sup>\*</sup>

F. D'Ammando<sup>1,2</sup>, G. Pucella<sup>1</sup>, C. M. Raiteri<sup>3</sup>, M. Villata<sup>3</sup>, V. Vittorini<sup>1,4</sup>, S. Vercellone<sup>5</sup>, I. Donnarumma<sup>1</sup>, F. Longo<sup>6</sup>, M. Tavani<sup>1,2</sup>, A. Arvan<sup>1</sup>, G. Barbiellini<sup>6</sup>, F. Boffelli<sup>7,8</sup>, A. Bulgarelli<sup>9</sup>, P. Caraveo<sup>10</sup>, P. W. Cattaneo<sup>7</sup>, A. W. Chen<sup>4,10</sup>, V. Cocco<sup>1</sup>, E. Costa<sup>1</sup>, E. Del Monte<sup>1</sup>, G. De Paris<sup>1</sup>, G. Di Cocco<sup>9</sup>, Y. Evangelista<sup>1</sup>, M. Feroci<sup>1</sup>, A. Ferrari<sup>11</sup>, M. Fiorini<sup>10</sup>, T. Froyland<sup>2,4</sup>, F. Fuschino<sup>9</sup>, M. Galli<sup>12</sup>, F. Gianotti<sup>9</sup>, A. Giuliani<sup>10</sup>, C. Labanti<sup>9</sup>, I. Lapshov<sup>1</sup>, F. Lazzarotto<sup>1</sup>, P. Lipari<sup>13</sup>, M. Marisaldi<sup>9</sup>, S. Mereghetti<sup>10</sup>, A. Morselli<sup>14</sup>, L. Pacciani<sup>1</sup>, A. Pellizzoni<sup>15</sup>, F. Perotti<sup>10</sup>, G. Piano<sup>1,2</sup>, P. Picozza<sup>14</sup>, M. Pilia<sup>15</sup>, M. Prest<sup>16</sup>, M. Rapisarda<sup>17</sup>, A. Rappoldi<sup>7</sup>, S. Sabatini<sup>1,2</sup>, P. Soffitta<sup>1</sup>, M. Trifoglio<sup>9</sup>, A. Trois<sup>1</sup>, E. Vallazza<sup>6</sup>, A. Zambra<sup>1</sup>, D. Zanello<sup>13</sup>, I. Agudo<sup>18</sup>, M. F. Aller<sup>19</sup>, H. D. Aller<sup>19</sup>, A. A. Arkharov<sup>20</sup>, U. Bach<sup>21</sup>, E. Benitez<sup>22</sup>, A. Berdyugin<sup>23</sup>, D. A. Blinov<sup>24</sup>, C. S. Buemi<sup>25</sup>, W. P. Chen<sup>26,27</sup>, A. Di Paola<sup>28</sup>, G. Di Rico<sup>29</sup>, D. Dultzin<sup>22</sup>, L. Fuhrmann<sup>21</sup>, J. L. Gómez<sup>18</sup>, M. A. Gurwell<sup>30</sup>, S. G. Jorstad<sup>31</sup>, J. Heidt<sup>32</sup>, D. Hiriart<sup>33</sup>, H. Y. Hsiao<sup>27</sup>, G. Kimeridze<sup>34</sup>, T. S. Konstantinova<sup>24</sup>, E. N. Kopatskaya<sup>24</sup>, E. Koptelova<sup>26,27</sup>, O. Kurtanidze<sup>34</sup>, V. M. Larionov<sup>20,24</sup>, P. Leto<sup>35</sup>, E. Lindfors<sup>23</sup>, J. M. Lopez<sup>33</sup>, A. P. Marscher<sup>31</sup>, I. M. McHardy<sup>36</sup>, D. A. Melnichuk<sup>24</sup>, M. Mommert<sup>32</sup>, R. Mujica<sup>37</sup>, K. Nilsson<sup>23</sup>, M. Pasanen<sup>23</sup>, M. Roca-Sogorb<sup>18</sup>, M. Sorcia<sup>22</sup>, L. O. Takalo<sup>23</sup>, B. Taylor<sup>38</sup>, C. Tringilio<sup>25</sup>, I. S. Troitsky<sup>24</sup>, G. Umam<sup>25</sup>, L. A. Antonelli<sup>39</sup>, S. Colafrancesco<sup>39</sup>, S. Cutini<sup>39</sup>, D. Gasparrini<sup>39</sup>, C. Pittori<sup>39</sup>, B. Preger<sup>39</sup>, P. Santolamazza<sup>39</sup>, F. Verrecchia<sup>39</sup>, P. Giommi<sup>39</sup>, L. Salotti<sup>40</sup>

(Affiliations can be found after the references)

received; accepted

## ABSTRACT

**Context.** We report the detection by the AGILE satellite of a rapid  $\gamma$ -ray flare from the source 1AGL J1511–0908, associated with the powerful  $\gamma$ -ray quasar PKS 1510–089, during a pointing centered on the Galactic Center region from 1 March to 30 March 2008. This source has been continuously monitored in the radio-to-optical bands by the GLAST-AGILE Support Program (GASP) of the Whole Earth Blazar Telescope (WEBT). Moreover, the  $\gamma$ -ray flaring episode triggered three ToO observations by the *Swift* satellite in three consecutive days, starting from 20 March 2008.

**Aims.** The quasi-simultaneous radio-to-optical, UV, X-ray and  $\gamma$ -ray coverage allows us to study in detail the multifrequency time evolution, the spectral energy distribution of this source and its theoretical interpretation based on the synchrotron and inverse Compton (IC) emission mechanisms.

**Methods.** During the radio-to-optical monitoring provided by the GASP–WEBT, AGILE observed the source with its two co-aligned imagers, the Gamma-Ray Imaging Detector (GRID) and the hard X-ray imager (SuperAGILE), sensitive in the 30 MeV–30 GeV and 18–60 keV energy bands, respectively.

**Results.** In the period 1–16 March 2008, AGILE detected  $\gamma$ -ray emission from PKS 1510–089 at a significance level of  $6.2\text{-}\sigma$  with an average flux over the entire period of  $(84 \pm 17) \times 10^{-8}$  photons  $\text{cm}^{-2} \text{s}^{-1}$  for photon energies above 100 MeV. After a predefined satellite re-pointing, between 17 and 21 March 2008, AGILE detected the source at a significance level of  $7.3\text{-}\sigma$ , with an average flux ( $E > 100$  MeV) of  $(134 \pm 29) \times 10^{-8}$  photons  $\text{cm}^{-2} \text{s}^{-1}$  and a peak level of  $(281 \pm 68) \times 10^{-8}$  photons  $\text{cm}^{-2} \text{s}^{-1}$  with daily integration. During the observing period January–April 2008, the source also showed an intense and variable optical activity, with several flaring episodes and a significant increase of the flux was observed at millimetric frequencies. Moreover, in the X-ray band the *Swift*/XRT observations seem to show an harder-when-brighter behaviour of the source spectrum.

**Conclusions.** The flat spectrum radio quasar PKS 1510–089 showed strong activity between January and April 2008, with episodes of rapid variability from radio to  $\gamma$ -ray energy bands, in particular with a rapid  $\gamma$ -ray flaring episode. The spectral energy distribution of mid-March 2008 is modelled with a homogeneous one-zone synchrotron self Compton (SSC) emission plus contributions from inverse Compton scattering of external photons from both the accretion disc and the broad line region. Indeed, some features in the optical–UV spectrum seem to indicate the presence of Seyfert-like components, such as the little blue bump and the big blue bump.

**Key words.** gamma-rays: observations – mechanism: non-thermal – quasars: individual (PKS 1510-089)

## 1. Introduction

Send offprint requests to: F. D'Ammando, e-mail: [filippo.dammando@iasf-roma.inaf.it](mailto:filippo.dammando@iasf-roma.inaf.it)

\* The radio-to-optical data presented in this paper are stored in the GASP-WEBT archive; for questions regarding their availability, please contact the WEBT President Massimo Villata.

Blazars are a subclass of AGN characterized by the emission of strong non-thermal radiation across the entire electromagnetic spectrum, from radio to very high energies. Their observational properties include irregular, rapid and often very large variability, apparent super-luminal motion, flat radio spectrum,

high and variable polarization at radio and optical frequencies. These features are interpreted as the result of the emission of electromagnetic radiation from a relativistic jet that is viewed closely aligned to the line of sight (Blandford & Rees 1978, Urry & Padovani 1995). The Spectral Energy Distribution (SED) of blazars is typically double-humped with a first peak occurring in the IR/optical band in the so-called *red blazars* (including Flat Spectrum Radio Quasars, FSRQs, and Low-energy peaked BL Lacs, LBLs) and at UV/X-rays in the so-called *blue blazars* (including High-energy peaked BL Lacs, HBLs). The first peak is commonly interpreted as synchrotron radiation from high-energy electrons in a relativistic jet. The second component of the SED, peaking at MeV–GeV energies in *red blazars* and at TeV energies in *blue blazars*, is commonly interpreted as inverse Compton (IC) scattering of seed photons by relativistic electrons (Ulrich et al., 1997), although a different origin of high energy emission has been proposed in hadronic models (see e.g., Böttcher 2007, for a recent review).

PKS 1510–089 is a nearby ( $z=0.361$ ) radio-loud highly polarized quasar (HPQ) already detected also in the MeV–GeV energy band by the EGRET instrument on board *CGRO* (Hartman et al. 1992). The broadband spectrum of the source is representative of the class of FSRQ with the inverse Compton component dominated by the  $\gamma$ -ray emission and the synchrotron emission peaked around IR frequencies, even if it is clearly visible in this source a pronounced UV bump possibly due to the thermal emission from the accretion disk (Malkan & Moore 1986, Pian & Treves 1993).

PKS 1510–089 has been extensively observed and studied in the X-ray band by the satellites EXOSAT (Singh, Rao & Vahia 1990, Sambruna et al. 1994), GINGA (Lawson & Turner 1997), ROSAT (Siebert et al. 1998), ASCA (Singh, Shrader & George 1997) and Chandra (Gambill et al. 2003). The observed X-ray spectrum was very flat in the 2–10 keV band with photon index of  $\Gamma \simeq 1.3$ , but it was steeper ( $\Gamma \simeq 1.9$ ) in the ROSAT band-pass (0.1–2.4 keV), suggesting the presence of a possible spectral break around 1–2 keV. The difference of the photon indices could be due to the presence of a soft X-ray excess. Observations by BeppoSAX (Tavecchio et al. 2000) confirm a possible presence of a soft X-ray excess below 1 keV. Evidences of a similar soft X-ray excess has been detected in other blazars such as 3C 273, 3C 279, AO 0235+164 and 3C 454.3, even if the origin of this excess is still an open issue.

During August 2006, PKS 1510–089 was observed in a relatively bright state by *Suzaku* over approximately three days and with *Swift* 10 times during 18 days as a Target of Opportunity (ToO) with a total duration of 24.3 ks. *Suzaku* measured a very hard X-ray spectrum ( $\Gamma < 1.5$ ), which seems to exclude models in which X-rays are produced by synchrotron radiation of the secondary ultrarelativistic population of electrons and positrons, as predicted by hadronic models. The *Swift*/XRT observations instead revealed significant spectral evolution in the 0.3–10 keV energy band on timescales of one week, with the spectrum that becomes harder as the source gets brighter (Kataoka et al. 2008).

Gamma-ray emission from PKS 1510–089 was detected several times by EGRET with a integrated flux above 100 MeV between  $(13 \pm 5)$  and  $(49 \pm 18) \times 10^{-8}$  photons  $\text{cm}^{-2} \text{s}^{-1}$  and an energy spectrum, integrated over all the EGRET observations, modelled with a power law with photon index  $\Gamma = 2.47 \pm 0.21$  (Hartman et al. 1999).

In August 2007, AGILE detected an intense  $\gamma$ -ray activity from PKS 1510–089. In particular, during the period 28 August – 1 September 2007 the average  $\gamma$ -ray flux observed was  $F_{E>100\text{MeV}} = (195 \pm 30) \times 10^{-8}$  photons  $\text{cm}^{-2} \text{s}^{-1}$  (Pucella et al.

2008). Recently, this source was detected again during high  $\gamma$ -ray activity states by both the Large Area Telescope (LAT) on board the *Fermi* GST (Ciprini et al. 2008, Tramacere 2009 and Cutini et al. 2009) and AGILE (D'Ammando et al. 2009, Pucella et al. 2009 and Vercellone et al. 2009). The results of the AGILE observations during March 2009 will be published in a forthcoming paper (D'Ammando et al., in preparation).

In this paper we present the analysis of the AGILE data obtained during the observations of PKS 1510–089 from 1 March 2008 to 30 March 2008 (see also D'Ammando et al. 2008a). We also present the radio-to-optical monitoring of the GASP-WEBT during the period January–April 2008, and the results of three *Swift* ToO carried out between 20 and 22 March 2008. This broadband coverage over the entire electromagnetic spectrum allows us to build and study in detail the spectral energy distribution of the source.

The paper is organized as follows. Section 2 describes the AGILE observations, and the corresponding data analysis. Section 3 introduces the *Swift* data and the relative analysis. Section 4 is dedicated to the results of the GASP-WEBT observations, while in Section 5 we discuss the spectral energy distribution, its implication for the emission mechanisms of the source, and finally we draw our conclusions.

Throughout this paper the quoted uncertainties are given at the  $1-\sigma$  level, unless otherwise stated, and the photon indices are parameterized as  $N(E) \propto E^{-\Gamma}$  (ph  $\text{cm}^{-2} \text{s}^{-1} \text{keV}^{-1}$  or  $\text{MeV}^{-1}$ ) with  $\Gamma = \alpha + 1$  ( $\alpha$  is the spectral index). We adopt a luminosity distance of  $d_L = 1915$  Mpc for PKS 1510-089, assuming  $z = 0.361$  and a  $\Lambda$ CDM cosmology with  $H_0 = 71 \text{ Km s}^{-1} \text{Mpc}^{-1}$ ,  $\Omega_m = 0.27$  and  $\Omega_\Lambda = 0.73$ .

## 2. AGILE Data

### 2.1. Observation of PKS 1510–089

The AGILE satellite (Tavani et al. 2008a,b) is an Italian Space Agency (ASI) Mission devoted to high-energy astrophysics, with four active detectors capable of observing cosmic sources simultaneously in X-ray and  $\gamma$ -ray energy bands.

The Gamma-Ray Imaging Detector (GRID) consists of a combination of a pair-production Silicon Tracker (ST; Prest et al. 2003, Barbiellini et al. 2001), sensitive in the energy range 30 MeV–30 GeV, a non-imaging CsI(Tl) Mini-Calorimeter (MCAL; Labanti et al. 2009) sensitive in the 0.3–100 MeV energy band, and a segmented Anti-Coincidence System (ACS) made of plastic scintillator layers which surrounds all active detectors (Perotti et al. 2006). A co-aligned coded-mask hard X-ray imager (SuperAGILE; Costa et al. 2001, Feroci et al. 2007) ensures coverage in the 18–60 keV energy band.

The AGILE observations of PKS 1510-089 were performed from 1 March 2008 12:45 UT to 21 March 2008 2:04 UT, for a total of 211 hours of effective exposure time. In the first period, between 1 and 16 March, the source was located  $\sim 50^\circ$  off the AGILE pointing direction. In the second period, between 17 March and 21 March, after a satellite re-pointing, the source was located at  $\sim 40^\circ$  off-axis. Finally, after a gap of 4 days of observation due to technical maintenance of the satellite, the source was observed at  $\sim 50^\circ$  off axis between 25 March 13:09 UT and 30 March 10:29 UT. Unfortunately during the observation the source was substantially off-axis in the field of view of SuperAGILE.

## 2.2. Data reduction and analysis

AGILE-GRID data were analyzed, starting from the Level-1 data, using the AGILE Standard Analysis Pipeline (see Vercellone et al. 2008 for a detailed description of the AGILE data reduction). An ad-hoc implementation of the Kalman Filter technique is used for track identification and event-direction reconstruction in detector coordinates and subsequently a quality flag is assigned to each GRID event, depending on whether it is recognised as a confirmed gamma-ray event, a charged particle event, a single-track event, or of uncertain nature.

After the creation of the event files, the AGILE Scientific Analysis Package can be run. Counts, exposure, and Galactic background  $\gamma$ -ray maps were generated with a bin-size of  $0.25^\circ \times 0.25^\circ$  for photons with energy  $E > 100$  MeV.

To reduce the particle background contamination, we selected only events flagged as confirmed  $\gamma$ -ray events, and all events collected during the South Atlantic Anomaly were rejected. We also rejected all the  $\gamma$ -ray events whose reconstructed directions form angles with the satellite-Earth vector smaller than  $80^\circ$ , in order to reduce the  $\gamma$ -ray Earth albedo contamination. The most recent version (BUILD-16) of the Calibration files at the time of writing, publicly available at the ASI Science Data Center (ASDC) site<sup>1</sup>, and of the  $\gamma$ -ray diffuse emission model (Giuliani et al. 2004) is used. We ran the AGILE maximum likelihood procedure with a radius of analysis of  $10^\circ$ , on the whole observing period, in order to obtain the average flux in the  $\gamma$ -ray band and estimate the diffuse parameters used also for measure the daily fluxes, according to the procedure described in Mattox et al. (1993).

## 2.3. Results

During the period 2008 March 1–16, AGILE-GRID detected  $\gamma$ -ray emission from a position consistent with the powerful  $\gamma$ -ray quasar PKS 1510–089 at a significance level of  $6.2\text{-}\sigma$  with an average flux over the entire period of  $(84 \pm 17) \times 10^{-8}$  photons  $\text{cm}^{-2} \text{s}^{-1}$  for photon energies above 100 MeV.

Instead, in the period 2008 March 17–21, AGILE detected  $\gamma$ -ray emission from a position consistent with the source at a significance level of  $7.3\text{-}\sigma$ . The AGILE 95% maximum likelihood contour level baricentre of the source is  $l = 351.49^\circ$ ,  $b = 40.07^\circ$ , with a distance between this position and the radio position ( $l = 351.29^\circ$ ,  $b = 40.14^\circ$ ) of  $0.17^\circ$ . The overall AGILE error circle, taking both statistical and systematic effects into account, has a radius  $r = 0.50^\circ$ . The average flux above 100 MeV during this second period, with the source located  $\sim 40^\circ$  off the AGILE pointing direction, was  $(134 \pm 29) \times 10^{-8}$  photons  $\text{cm}^{-2} \text{s}^{-1}$ . The peak level of activity with daily integration was  $(281 \pm 68) \times 10^{-8}$  photons  $\text{cm}^{-2} \text{s}^{-1}$ , showing an increase of a factor two in one day and at least three in two days, as the source had not been detected for some days after two episodes of medium intensity. After the sudden increase, the flux rapidly decreased around March 19, 2008.

Fitting the data relative to the period March 17–21 with a simple power law model we obtain a photon index of  $\Gamma = 1.81 \pm 0.34$ . This photon index is calculated with the weighted least squares method, considering for the fit three energy bins: 100–200 MeV, 200–400 MeV and 400–1000 MeV. The photon index obtained for this second period is consistent within the errors with the one observed by AGILE in August 2007 ( $\Gamma = 1.98 \pm 0.27$ ).

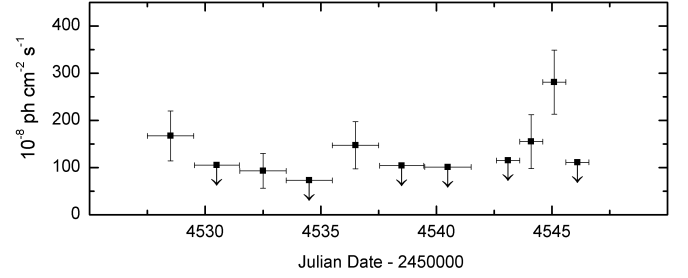


**Fig. 1.** AGILE-GRID  $\gamma$ -ray light curve between 1 and 21 March 2008 at 1-day or 2-day resolution for  $E > 100$  MeV with fluxes in units of  $10^{-8}$  photons  $\text{cm}^{-2} \text{s}^{-1}$ . The downward arrows represent  $2\text{-}\sigma$  upper limits.

Figure 1 shows the  $\gamma$ -ray light-curve between 1 and 21 March 2008 with 2-day resolution for the first period and 1-day for the second period, for photons of energy above 100 MeV. The downward arrows represent  $2\text{-}\sigma$  upper limits. Upper limits are calculated when the analysis provides a significance of detection  $< 3\text{-}\sigma$  (see Mattox et al. 1996).

Finally, in the third period between 25 and 30 March 2008 the source was not detected by the GRID and an upper limit with 95% confidence level of  $54 \times 10^{-8}$  photons  $\text{cm}^{-2} \text{s}^{-1}$  is provided.

During August–October 2008, *Fermi*-LAT detected the source with an average flux for  $E > 100$  MeV of  $(55.8 \pm 3.3) \times 10^{-8}$  photons  $\text{cm}^{-2} \text{s}^{-1}$  and a peak of intensity of  $(165.9 \pm 11.7) \times 10^{-8}$  photons  $\text{cm}^{-2} \text{s}^{-1}$  (Abdo et al. 2009). The peak of  $\gamma$ -ray emission corresponds to the first flare observed by *Fermi*-LAT at the end of September 2008 (Tramacere 2008); the average flux value confirms the flaring state observed by AGILE in mid-March.

Moreover in August–October 2008, *Fermi*-LAT observed a softer photon index for this source,  $\Gamma = 2.48 \pm 0.05$  (Abdo et al. 2009), but this value corresponds to an average value over three months of observation in which the source flux was variable, whereas the value reported by us refers to a rapid flaring episode. The value obtained by *Fermi*-LAT is very similar to that measured by EGRET averaging over all the observations ( $\Gamma = 2.47 \pm 0.21$ ), confirming that the average spectral indexes are softer than those measured during short flaring states. The difference between the value obtained by AGILE and *Fermi* could also be partially due to the different bandpasses of the two instruments.

## 3. SWIFT observations

The NASA *Swift* gamma-ray Burst Mission (Gehrels et al. 2004), performed three ToO observations of PKS 1510–089 in three consecutive days with the first occurring on 20 March 2008. The three observations were performed using all three on-board experiments: the X-ray Telescope (XRT; Burrows et al. 2005, 0.2–10 keV), the UV and Optical Telescope (UVOT; Roming et al. 2005, 170–600 nm) and the coded-mask Burst Alert Telescope (BAT; Barthelmy et al. 2005, 15–150 keV). The hard X-ray flux of this source is below the sensitivity of the BAT instrument for so short exposure and therefore the data from this instruments will not be used.

### 3.1. Swift/XRT Data

The XRT data were processed with standard procedures (xrtpipeline v0.12.0), the filtering and screening criteria were

<sup>1</sup> <http://agile.asdc.asi.it>

**Table 1.** Observation log and fitting results of *Swift*/XRT observations of PKS 1510-089. Power law model with  $N_H$  fixed to Galactic absorption. <sup>a</sup> Unabsorbed flux. <sup>b</sup> Cash statistic (C-stat) and percentage of Montecarlo realizations that had statistic < C-stat, performing  $10^4$  simulations.

Observation Date	Exposure Time (sec)	Counts (0.2 - 10 keV)	Flux 0.3-10 keV <sup>a</sup> erg cm <sup>-2</sup> s <sup>-1</sup>	Photon index $\Gamma$	$\chi^2_{red}$ (d.o.f.) / C-stat (%) <sup>b</sup>
20-Mar-2008	1961	306	$12.20^{+1.65}_{-1.65} \times 10^{-12}$	$1.16 \pm 0.16$	0.87 (13)
21-Mar-2008	1966	189	$8.77^{+1.35}_{-1.39} \times 10^{-12}$	$1.53 \pm 0.17$	467 (48.2) <sup>b</sup>
22-Mar-2008	1885	261	$9.48^{+1.13}_{-1.14} \times 10^{-12}$	$1.41 \pm 0.19$	1.34 (11)

applied by means of the FTOOLS in the Heasoft package v6.5. Given the low rate of PKS 1510-089 during the three observations ( $< 0.5$  count s<sup>-1</sup> in the 0.2–10 keV range), we only considered photon counting (PC) data for our analysis, and further selected XRT grades 0–12 (according to *Swift* nomenclature, see Burrows et al. 2005). No pile up correction was necessary. The ancillary response files were generated with the task `xrtmkarf`, applying corrections for the PSF losses and CCD defects, and we used the latest spectral redistribution matrices (RMF, v011) in the Calibration Database maintained by HEASARC. The adopted energy range for spectral fitting is 0.3–10 keV and all data were rebinned with a minimum of 20 counts per energy bin to use the  $\chi^2$  minimization fitting technique. An exception is the observation of 2008 March 21, when the number of counts was so low that the Cash statistic (Cash, 1979) on ungrouped data was used. *Swift*/XRT uncertainties are given at 90% confidence level for one interesting parameter, unless otherwise stated.

Spectral analysis was performed using the XSPEC fitting package 12.4.0 (Arnaud et al. 1996). We fitted the spectra with a power law model with Galactic absorption fixed to  $N_H = 6.89 \times 10^{20}$  cm<sup>-2</sup> (Kalberla et al. 2005). Table 1 summarizes the most important information on XRT observations and the relative spectral fit parameters.

A variability of about 30% in the X-ray flux of the source was observed on time scale of one day. Notwithstanding the uncertainties due to the errors on fluxes and photon indexes, the XRT data seem to indicate that the X-ray spectrum becomes harder when the source gets brighter, confirming the behaviour already observed in this source by Kataoka et al. (2008) during the *Swift*/XRT observations carried out in August 2006. This is a trend often observed in HBL (see e.g. Massaro et al. 2008, Tramacere et al. 2007, Kataoka et al. 1999), but quite rare for quasar-hosted blazars such as PKS 1510-089. For instance, 3C 454.3 shows approximately the same spectral slope in different brightness states (see e.g. Raiteri et al. 2007; Raiteri et al. 2008).

### 3.2. *Swift*/UVOT Data

During the three *Swift* pointings, the UVOT instrument (Poole et al. 2008) observed PKS 1510-089 in all its optical (*V*, *B*, and *U*) and UV (UVW1, UVM2, and UVW2) photometric bands. Data were reduced with the `uvotmaghist` task of the HEASOFT package. Source counts were extracted from a circular region of 5 arcsec radius, centred on the source, while the background was estimated from a surrounding annulus with 8 and 18 arcsec radii. In the first two days only one exposure per filter was available, while three exposures per filter were acquired in the last day. With the only exception of UVM2, the source brightness resulted quite stable in all the UVOT bands, with variations of a few hundredth of mag, well inside the typical UVOT data uncertainty of 0.1 mag due to both systematic and statistical errors. Average values are: *V* = 16.94, *B* = 17.19,

*U* = 16.31, UVW1 = 16.64, and UVW2 = 16.55. The UVM2 frames have low signal-to-noise ratios, thus the source magnitude in this band presents a larger dispersion; the average value is *UVM2* =  $16.47 \pm 0.14$ .

## 4. Radio-to-optical observations by the GASP

PKS 1510-089 is one of the 28  $\gamma$ -ray-loud blazars that are regularly monitored by the GLAST-AGILE Support Program (GASP; Villata et al. 2008) of the Whole Earth Blazar Telescope (WEBT). Optical and near-IR data are collected as already calibrated magnitudes, according to a common choice of photometric standards from Raiteri et al. (1998). Radio data are provided as calibrated flux densities. The reference optical band for the GASP is the *R* band; the corresponding light curve in January–April 2008 is shown in the top panel of Fig. 1, with the data provided by the following observatories: Abastumani, Calar Alto<sup>2</sup>, Crimean, Lowell (Perkins), Lulin, Roque de los Muchachos (KVA and Liverpool), San Pedro Martir, St. Petersburg, Torino. The source showed intense activity during all the considered period, with several episodes of fast variability. At the beginning of the optical observing season, the January observations indicate that the source was in a faint state, around *R* = 16.6. A fast brightening of  $\sim 1.3$  mag in 8 days led the source to *R* = 15.3 on February 15. This was followed by a  $\sim 0.6$  mag dimming in 4 days. Other minimum brightness states were observed on March 23 and in late April, while peaks were detected on March 29 and April 11. Near-IR data in the *JHK* bands were taken at Campo Imperatore and Roque de los Muchachos (Liverpool). Millimetric flux densities at 345 and 230 GHz came from the Submillimeter Array (SMA) on Mauna Kea. Centimetric radio data were acquired at Medicina (22 and 8 GHz), Noto (43 GHz), and UMRAO (14.5, 8.0, and 4.8 GHz). In Fig. 1 the source radio behaviour in different bands is compared to the optical one (top panel). The light curve at high radio frequencies (230–345 GHz) suggests that the mechanism producing the flaring events observed in the optical band in the second half of February and in late March–April 2008 also interested the millimetric emitting zone, with some delay. An estimate of this delay is hampered by the limited data sampling. At lower radio frequencies (22–43 GHz) a hint of flux increase is visible in the second part of the light curve, while the radio flux at 5–15 GHz shows no trend. This suggests that the jet regions that are responsible for the emission at the longest radio wavelengths are not affected by the flaring mechanism.

<sup>2</sup> Calar Alto data were acquired as part of the MAPCAT (Monitoring AGN with Polarimetry at the Calar Alto Telescopes) project.

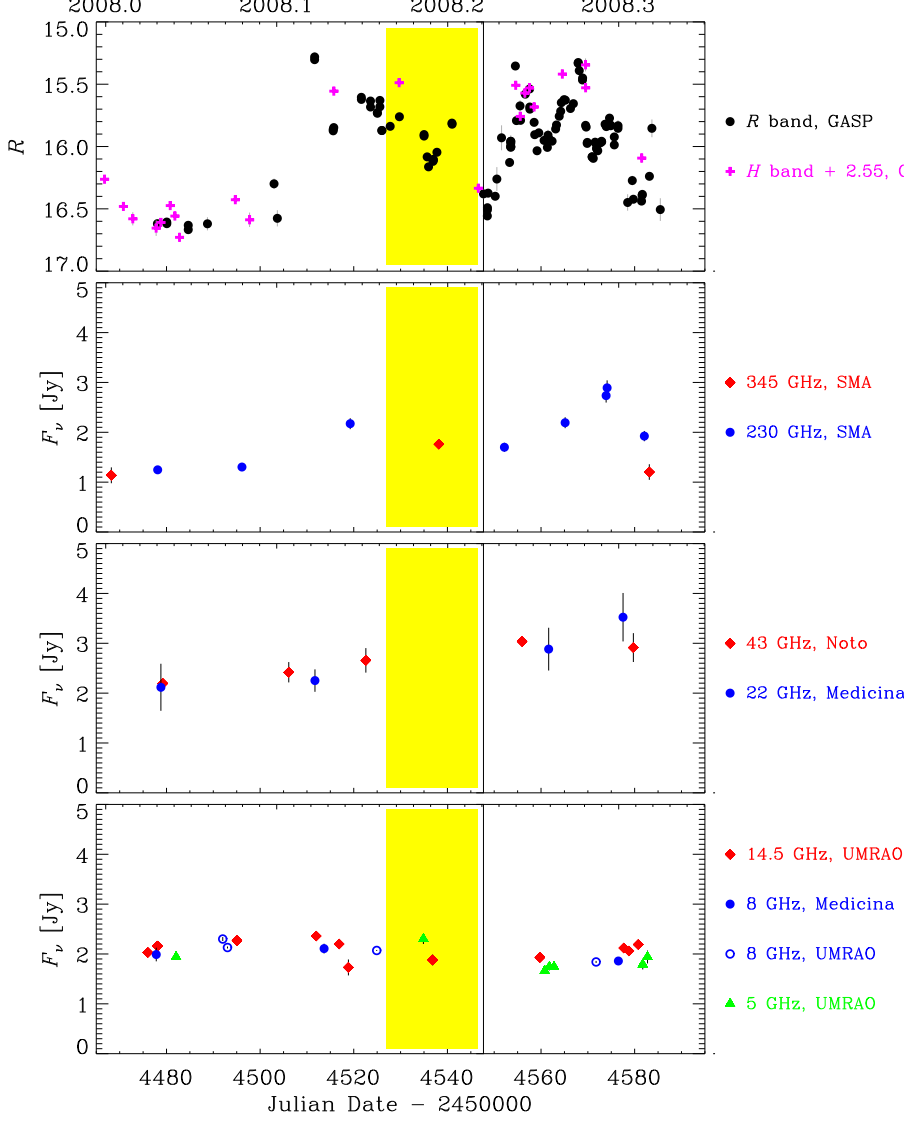


**Fig. 2.** Optical light curve of PKS 1510-089 (top panel) obtained by the GASP-WEBT during the period January-April 2008 compared to its radio flux densities at different frequencies. The vertical bar indicates the time of the *Swift* observations. The yellow shaded region marks the period also covered by the AGILE observation.

## 5. Discussion and conclusions

In the last two years, PKS 1510–089 showed a very high activity in  $\gamma$ -ray band with several flaring episodes (see Pucella et al. 2008, Tramacere 2008, Ciprini et al. 2009, D’Ammando et al. 2009, Pucella et al. 2009, Vercellone et al. 2009 and Cutini et al. 2009). During the period January–April 2008, the source showed a high variability over all the electromagnetic spectrum from radio to  $\gamma$ -rays, with several flaring episodes in the optical band and a rapid and intense flare detected in the  $\gamma$ -ray band in mid-March.

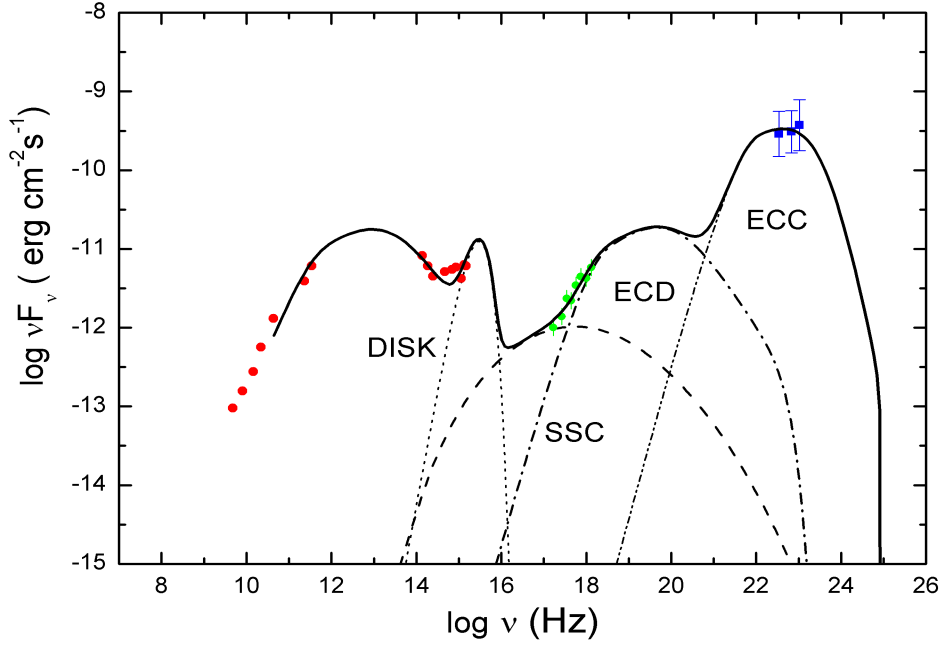
### 5.1. Modelling the Spectral Energy Distribution

Figure 3 shows the spectral energy distribution for the AGILE-GRID observation period 2008 March 17–21, including quasi-simultaneous optical and radio data by GASP, and UVOT and X-ray data by *Swift*. Since the source brightness over the three days of UVOT observations remained stable, we built a unique SED for the whole period, including contemporaneous data at other frequencies, in particular radio-to-optical data from the GASP. The optical and near-IR data were acquired exactly in the period of the UVOT observations: one *R*-band datum from

Roque (KVA) and *J*, *H*, and *K* data from Campo Imperatore. The UVOT and GASP magnitudes were corrected for Galactic extinction by adopting  $A_B = 0.416$  mag, and deriving the values in the other bands according to Cardelli et al. (1989). To convert magnitudes into fluxes, we assumed the zero-mag fluxes by Poole et al. (2008) and Bessel et al. (1998).

Radio light curves are less well-sampled than the *R*-band one (see Fig. 2); the high-frequency radio data (43–345 GHz) shown in the SED were taken within a week from the UVOT observations, while the low-frequency data points were obtained by interpolating between the closest data preceeding and following the UVOT observations. This is justified by the smooth behaviour of the low-frequency radio light curves.

The dip in the SED corresponding to the UVW1 frequency must be regarded with cautious, since it is also found for other blazars with different redshift and could be systematic. Observations performed by *Swift* and the GASP in March and June 2007, when the source was nearly at the same brightness level, showed the same shape in the near-IR-to-UV part of the SED. A similar trend characterized the optical–UV SED of August 2006 shown by Kataoka et al. (2008). We notice that the shape of the SED in the optical band may be affected by the



**Fig. 3.** Spectral Energy Distribution of PKS 1510-089 for the AGILE-GRID observation of 17–21 March 2008, including quasi-simultaneous GASP radio-to-optical data, the *Swift*/UVOT data of 20–22 March and the *Swift*/XRT data of 20 March. The dotted, dashed, dot-dashed and double-dot-dashed lines represent the accretion disk black body, the SSC, the ECD and the ECC radiation, respectively.

flux contribution of broad emission lines, including the little blue bump (Neugebauer et al. 1979, Smith et al. 1988).

For the SED we used the *Swift*/XRT data collected on 20 March, the observation closest to the  $\gamma$ -ray flare and during which the higher X-ray flux was observed.

In order to model the spectral energy distribution we used a homogeneous one-zone synchrotron self Compton (SSC; Marscher & Gear 1985, Maraschi et al. 1992, Bloom & Marscher 1996) model, plus the contribution of external Compton scattering of both direct disk radiation (ECD; Dermer et al. 1992) and photons from the broad line region (BLR) clouds (ECC; Sikora et al. 1994). The strong thermal features usually observed in FSRQs (and in this blazars in particular, see Neugebauer et al. 1978, Smith et al. 1988) at optical/UV frequencies suggest that the environment is rich of soft photons produced by the accretion disk and/or reprocessed by the BLR. This implies that the energy density of the external soft radiation is much higher than that of the synchrotron radiation, therefore during the  $\gamma$ -ray flares in FSRQs the most important processes are the ECC and ECD and the  $\gamma$ -ray photon index could be determined by the dominant contribution of the two.

We consider a moving spherical blob of radius  $R$ , filled by relativistic electrons and embedded in a random magnetic field. We assume that the electron energy density distribution is described by a broken power law:

$$n_e(\gamma) = \frac{K\gamma_b^{-1}}{(\gamma/\gamma_b)^{p_1} + (\gamma/\gamma_b)^{p_2}} \quad (1)$$

where  $\gamma$  is the electron Lorentz factor assumed to vary between  $\gamma_{\min}$  and  $\gamma_{\max}$ ,  $p_1$  and  $p_2$  are pre- and post-break electron distribution spectral indexes, respectively, and  $\gamma_b$  is the break energy Lorentz factor. We assume that the blob contains a comoving random average magnetic field  $B$  with a bulk Lorentz factor  $\Gamma$

Parameter	Value	Units
$p_1$	2.2	
$p_2$	4.6	
$\gamma_{\min}$	30	
$\gamma_b$	290	
$\gamma_{\max}$	5200	
$K$	75	$\text{cm}^{-3}$
$R$	10	$10^{15} \text{ cm}$
$B$	3.5	G
$\delta$	20.26	
$L_d$	5	$10^{45} \text{ erg s}^{-1}$
$\theta$	2.86	degrees
$\Gamma$	18	

**Table 2.** Parameters for the model used to explain the SED of PKS 1510-089 during the  $\gamma$ -ray flare of March 18-19, 2008.

at an angle  $\theta$  with respect to the line of sight. The relativistic Doppler beaming factor is then  $\delta = [\Gamma(1-\beta\cos\theta)]^{-1}$ , and  $K$  is the normalization density parameter into the blob.

We have chosen an angle of view of 0.05 rad in agreement with both the apparent jet velocities derived from multiepoch Very Long Baseline Array (VLBA) observations of the source (Homan et al. 2001; Wardle et al. 2005; Jorstad et al. 2005; Lister et al. 2009) and the value used by Kataoka et al. (2008).

The short time variability observed in  $\gamma$ -ray band constrains the size of the emitting region to  $R < c\Delta t_{\text{var}}\delta/(1+z) = 3.86 \times 10^{16} \text{ cm}$ , where  $\Delta t_{\text{var}}$  is the observed variation time. An accretion disk characterized by a black body spectrum with a luminosity of  $5 \times 10^{45} \text{ erg s}^{-1}$ , as estimated with UV observations by Pian & Treves (1993), at 0.05 pc from the blob is assumed as one of the sources of external target photons. We also assumed a BLR at 0.2 pc, reprocessing 10% of the irradiating continuum. The IC



spectra derived from the approximation of the BLR radiation as a black body reproduces quite well more refined spectra calculated by Tavecchio et al. (2008) taking into account a more accurate shape of the BLR.

Assuming a model with synchrotron, SSC and EC components plus the contribution from the accretion disk radiation, the spectral energy distribution of mid March 2008 can be well represented with input parameters summarized in Table 2. In the choice of the parameters we were guided by the knowledge of the angle of view, the disc luminosity and the simultaneous observations of the synchrotron and IC peak regions (therefore of the synchrotron and IC peak frequencies and luminosities). In addition, the minimum variability timescale gives an indication of the size of the emitting region. However, even if these quantities are quite well tightly constrained by fitting the whole SED, the choice of some parameters is not unique because the contemporaneous presence of the synchrotron, SSC, ECC and ECD components leads to a possible partial degeneration of the parameters.

### 5.2. X-ray spectral evolution

The spectral evolution detected in X-rays by *Swift* in just two days, soon after the  $\gamma$ -ray flaring episode is another hint of the rapid change of activity of this source. Usually in FSRQs as PKS 1510-089 only little variability is observed in X-rays on short timescales from hours to days, and also on longer timescales the X-ray spectral shape is almost constant with only little variations. The photon indices measured by *Swift*/XRT in March 2008, in particular during the first observation, tend to be lower than usually observed in FSRQs ( $\langle \Gamma_{[0.1-2.4]} \rangle = 1.76 \pm 0.06$  and  $\langle \Gamma_{[2-10]} \rangle = 1.65 \pm 0.04$ , Donato et al. 2001) and are more similar to those observed in some high redshift quasars (such as RBS 315, Tavecchio et al. 2007, and Swift J0746+2548, Sambruna et al. 2007). The hard photon indices of high redshift blazars could be interpreted in terms of absorption by warm plasma in the region surrounding the source, in agreement with a scenario where in the early evolution phases the quasars are substantially obscured by gas subsequently expelled from the host galaxy by powerful winds (see e.g. Fabian 1999). However, considering the low redshift, this interpretation is unlikely for this source.

Instead the X-ray spectral evolution observed by *Swift*/XRT could be due to the contamination of an additional component below  $\sim 2$  keV: the soft X-ray excess. In fact previous observations with Chandra (Gambill et al. 2004) and Suzaku (Kataoka et al. 2008) seem to indicate the presence of the soft X-ray excess in the spectrum of PKS 1510-089. The soft X-ray excess is an emission in excess of the extrapolation of the power law component dominating at higher energies, but the origin of this excess in AGNs is still an open issue (see e.g. D’Ammando et al. 2008b for a detailed discussion). In the past, it was often associated with the thermal emission of the accretion disc and then related to the big blue bump. However, it has recently been shown that modelling the soft X-ray excess in non-blazar AGNs with a thermal component yields a disc temperature remarkably constant, around 0.1–0.2 keV, regardless the central black hole mass and luminosity (Gierlinsky & Done 2004, Crummy et al. 2006). Also in Kataoka et al. (2008) the soft X-ray excess is tentatively described by a black body with temperature  $kT \approx 0.2$  keV. This result is difficult to explain in any model for the soft excess related to disc continuum emission, as in any disc model the temperature is expected to vary with both the black hole mass and the accretion rates.

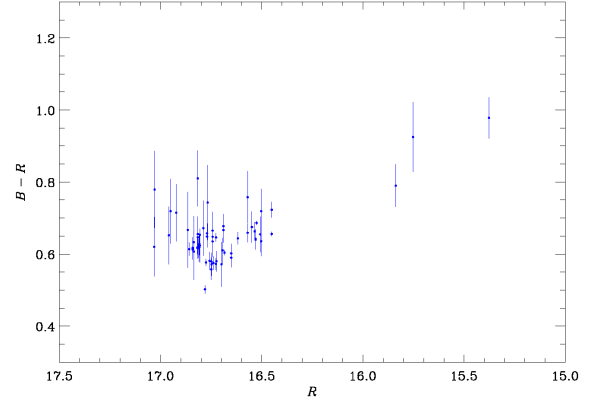


**Fig. 4.**  $B-R$  color index versus  $R$ -band magnitude for PKS 1510-089 obtained with archive data of the Torino Observatory.

For FSRQs one possible theoretical explanation is that the soft X-ray excess is a bulk Comptonization feature produced by cold plasma accelerated in a jet (Celotti et al. 2007), even if until now this feature has never been positively observed; in BL Lac objects instead the radiative environment is too weak to produce the soft X-ray excess via bulk Compton and the soft X-ray excess is likely related to the high energy tail of the synchrotron emission.

The change of photon index observed during the *Swift*/XRT observations could be due to the fact that the spectral shape of the inverse Compton component in X-ray remains roughly constant, but the amount of contamination from the soft excess emission varies. The contribution of the soft X-ray excess would be more important when the source gets fainter, affecting the spectrum at higher energies. Unfortunately the brief exposure of the *Swift* observation does not allow a detailed spectral modelling of this feature.

A possibility for the origin of this hard power law in PKS 1510-089 is that the photon index observed in X-rays is due to the combination of the synchrotron self Compton and external Compton emission and therefore due to the mismatch of the spectral slopes of these two components, not to the presence of a real soft X-ray excess. This is the solution that the data presented in this paper would favour. In this context, the spectral evolution during the three *Swift*/XRT observations could be due to the change of contribution of one of the two components and therefore to a different variability of the SSC and EC components.

### 5.3. Thermal emission components

Even if the SED of the blazars are usually dominated by the beamed non-thermal jet radiation, some of them show the signature of features Seyfert-like as the little blue bump and the big blue bump. The little blue bump is usually observed in quasars between  $\sim 2000$  and  $\sim 4000$  Å in the rest frame and it is likely due to the contribution of FeII and MgII emission lines and the Balmer continuum produced in the Broad Line Region (Wills et al. 1985). The big blue bump instead is associated with a rise in the UV band commonly interpreted as thermal emission from the accretion disc (see e.g. Laor 1990). Evidences of these thermal components have been found in other quasar-like blazar as 3C 273 (Grandi and Palumbo 2004; Türler et al. 2006), 3C 279 (Pian et al. 1999) and 3C 454.3 (Raiteri et al. 2007).



The presence of the emission by the accretion disk is consistent with the scenario in which the seed photons for the IC producing the  $\gamma$ -rays are external to the relativistic jet but usually it is not observed because hidden by the beamed variable synchrotron emission. The fact that the synchrotron component of PKS 1510-089 peaks around  $10^{13}$  Hz (see Bach et al. 2007, Nieppola et al. 2008) allows us to observe these thermal features in this source. In fact around  $10^{15}$  Hz a rising emission is visible in the spectrum and it is likely a manifestation of the big blue bump produced by the accretion disk, as already discussed for this source by Malkan & Moore (1986) and Pian & Treves (1993); moreover a hint of the presence of the little blue bump seems to appear in the SED of the source at  $10^{14.5}$  Hz.

Given the redshift of PKS 1510-089, the  $H\alpha$ ,  $H\beta$ , FeII and MgII lines mostly contribute to the observed spectrum between  $10^{14.2}$  and  $10^{14.8}$  Hz, and together with the disc emission, could explain the excess of emission observed around  $10^{14.5}$  Hz and not modelled from the other components represented in the SED. Moreover the presence of these non-jet components in the blue part of the spectrum of this blazar has already been observed by Neugebauer et al. (1979) and Smith et al. (1988) and it is in agreement with the redder-when-brighter behaviour shown by the  $B - R$  index versus  $R$ -band plot of Fig. 4. The plot has been obtained with archive data stored at the Torino Observatory.

#### 5.4. Energetics and alternative model

Finally to estimate the energetics of PKS 1510-089 we compute the isotropic luminosity in the  $\gamma$ -ray band, comparing with the Eddington and bolometric luminosity and the total power transported by the jet. For a given source with redshift  $z$ , the isotropic emitted luminosity in the energy band  $\epsilon$  is defined as:

$$L(z)_\epsilon = \frac{4\pi F d_1^2(z)}{(1+z)^{(1-\alpha_\gamma)}}, \quad (2)$$

where, in our case,  $\epsilon$  is the  $\gamma$ -ray energy band with  $E_{\min} = 100$  MeV and  $E_{\max} = 10$  GeV,  $\alpha_\gamma = \Gamma - 1$ ,  $F$  is the  $\gamma$ -ray energy flux between  $E_{\min}$  and  $E_{\max}$  calculated from the photon flux  $F_\gamma$  ( $E > 100$  MeV) as suggested by Ghisellini et al (2009):

$$F = 1.6 \times 10^{-12} \frac{\alpha_\gamma F_\gamma}{1 - \alpha_\gamma} [100^{1-\alpha_\gamma} - 1] \quad (3)$$

The luminosity distance is given by

$$d_1(z_1, z_2) = (1 + z_2)^2 \times \frac{c/H_0}{1 + z_2} \int_{z_1}^{z_2} [E(z)]^{-1} dz, \quad (4)$$

where  $z_1 = 0$ ,  $z_2 = z_{\text{src}}$  and

$$E(z) = \sqrt{\Omega_m(1+z)^3 + (1 - \Omega_m - \Omega_\Lambda)(1+z)^2 + \Omega_\Lambda}, \quad (5)$$

where  $H_0$  is the Hubble constant,  $\Omega_m$  and  $\Omega_\Lambda$  are the contribution of the matter and of the cosmological constant, respectively, to the density parameter. Using a luminosity distance  $d_L = 1915$  Mpc and the average  $\gamma$ -ray flux observed by the AGILE-GRID during 17–21 March 2008, we obtain for PKS 1510-089 ( $z = 0.361$ ) an isotropic luminosity  $L_\gamma^{\text{iso}} = 5.3 \times 10^{47}$  erg s $^{-1}$ .

The power carried by the jet in the form of magnetic field ( $L_B$ ), cold protons ( $L_p$ ), relativistic electrons ( $L_e$ ) and produced radiation ( $L_{\text{rad}}$ ), are:

$$L_p = \pi R^2 \Gamma^2 c \int [N(\gamma) m_p c^2 d\gamma] = 3.6 \times 10^{45} \text{ erg s}^{-1} \quad (6)$$

$$L_e = \pi R^2 \Gamma^2 c \int [N(\gamma) \gamma m_e c^2 d\gamma] = 1.5 \times 10^{44} \text{ erg s}^{-1} \quad (7)$$

$$L_B = \pi R^2 \Gamma^2 c U_B = 1.5 \times 10^{45} \text{ erg s}^{-1} \quad (8)$$

$$L_{\text{rad}} \simeq L_{\text{iso}} \Gamma^2 / \delta^4 = 5.3 \times 10^{45} \text{ erg s}^{-1} \quad (9)$$

where  $U_B$  is the magnetic energy density. Therefore the total power transported by the jet is  $P = L_B + L_p + L_e + L_{\text{rad}} = 1.1 \times 10^{46}$  erg s $^{-1}$ .

Assuming for the source a black hole mass  $M_{\text{BH}} = 4.5 \times 10^8 M_\odot$  (Woo & Urry 2002), we obtain an Eddington luminosity

$$L_{\text{Edd}} = \frac{4\pi G c m_H}{\sigma_T} M_{\text{BH}} = 5.7 \times 10^{46} \text{ erg s}^{-1} \quad (10)$$

to be compared with the bolometric luminosity  $L_{\text{bol}} = 2.4 \times 10^{46}$  erg s $^{-1}$  reported in Woo & Urry (2002).

An alternative theoretical model was recently proposed by Kataoka et al. (2008) to interpret the data of PKS 1510-089 collected during August 2006, with the high energy emission originated by the Comptonization of infrared radiation produced by the molecular torus surrounding the central engine and suggesting that the soft X-ray excess could be produced by the IC scattering of external photons by a population of cold electrons, as discussed by Begelman et al. (1997) and Celotti et al. (2007). An accurate theoretical interpretation of the SED is beyond the scope of this paper; however, our data seem not to rule out this alternative model. Infact, we have not simultaneous observations in FIR band that can confirm the excess detected by IRAS (Tanner et al. 1996), interpreted by Kataoka et al. as due to dust radiation from the nuclear torus and assumed as main source of seed photons for the IC mechanism. Moreover, the bulk Comptonization feature should not be easily observable during a high activity state of the source, such as that observed in mid-March 2008, because overwhelmed by the SSC and ECD emission and therefore this is not the best situation to test this hypothesis.

Further X-ray observations with XMM-Newton and Suzaku, simultaneously with the optical monitoring by means of REM Telescope and WEBT Consortium, could give important indication of the emission mechanisms involved in this source, in particular of the real nature of the soft X-ray excess, the presence in the spectrum of Seyfert-like features and the existence of the bulk Comptonization feature or not.

Finally, with two  $\gamma$ -ray satellites, AGILE and Fermi, in orbit at the same time we will be able to study in detail the source behaviour at high energies on long time scale, even if a wide multiwavelength coverage is necessary to achieve a complete understanding of the structure of the jet, the origin of the seed photons for the inverse Compton process and all the emission mechanisms working in this blazar.

**Acknowledgements.** We thank the anonymous referee for the useful comments. The AGILE Mission is funded by the Italian Space Agency (ASI) with scientific and programmatic participation by the Italian Institute of Astrophysics (INAF) and the Italian Institute of Nuclear Physics (INFN). We acknowledge the use of public data from the Swift data archive. We thank Swift Team for making these observations possible, particularly the duty scientists and science planners. The Submillimeter Array is a joint project between the Smithsonian Astrophysical Observatory and the Academia Sinica Institute of Astronomy and Astrophysics and is funded by the Smithsonian Institution and the Academia Sinica. UMRAO is funded by a series of grants from the NSF and by the University of Michigan. The research has been supported by the Taiwan National Science Council grant No. 96-2811-M-008-058. This paper is partly based on observations carried out at the German-Spanish Calar Alto Observatory, which is jointly operated by the MPIA and the IAA-CSIC. Acquisition of the MAPCAT data is supported in part

by the Spanish “Ministerio de Ciencia e Innovación” through grant AYA2007-67626-C03-03. Some of the authors acknowledge financial support by the Italian Space Agency through contract ASI-INAF I/088/06/0 for the Study of High-Energy Astrophysics.

*Facilities:* AGILE, *Swift*, UMRAO and WEBT.

## References

- Abdo, A. A., Ackermann, M., Ajello, M., et al. 2009, *ApJ*, 700, 597
- Arnaud, K. A. 1996, “Astronomical Data Analysis Software and Systems V”, eds. Jacoby G. and Barnes J., ASP Conf. Series, 101, 17
- Bach, U., Raiteri, C. M., Villata, M., et al. 2007, *A&A*, 464, 175
- Barbiellini, G., et al. 2001, *Amer. Inst. Phys. Conf. Series*, Vol. 587, *Gamma 2001: Gamma-Ray Astrophysics*, ed. S. Ritz, N. Gehrels, & C. R. Shrader, 754
- Barthelmy, S. D., Barbier, L. M., Cummings, J. R., et al. 2005, *Space Science Reviews*, 120, 143
- Begelman, M. C., & Sikora, M. 1987, *ApJ*, 322, 650
- Bessell, M. S., Castelli, F., & Plez, B. 1998, *A&A*, 333, 231
- Blandford, R. D., & Rees, M. J. 1978, in *BL Lac Objects* ed A.M Wolfe (Univ. Pittsburgh Press), 328
- Bloom, S. D., & Marscher, A. P. 1996, *ApJ*, 461, 657
- Bolton, J. G., & Ekers, J. 1966, *Aust. J Phys.*, 19, 559
- Böttcher, M. 2007, *Ap&SS*, 309, 95
- Burbidge, E. M., & Kinnman, T. D. 1966, *ApJ*, 145, 654
- Burrows, D. N., Hill, J. E., Nousek, J. A., et al. 2005, *Space Science Reviews*, 120, 165
- Cardelli, J. A., Clayton, G. C., & Mathis, J. S. 1989, *ApJ*, 345, 245
- Cash, W., 1979, *ApJ*, 228, 939
- Celotti, A., Ghisellini, G., Fabian, A. C. 2007, *MNRAS*, 375, 417
- Ciprini, S., and Corbel, F. 2009, *ATel*, 1897
- Costa, E., et al. 2001, *X-ray Astronomy: Stellar Endpoints, AGN, and the Diffuse X-ray Background*, ed. N.E. White et al. (New York: AIP) 599, 582
- Crummey, J., Fabian, A. C., Gallo, L., et al. 2006, *MNRAS*, 365, 1067
- Cutini, S., and Hays, E. 2009, *ATel*, 2033
- D’Ammando, F., Bulgarelli, A., Vercellone, S., et al. 2008a, *ATel*, 1436
- D’Ammando, F., Bianchi, S., Jiménez-Bailón, E., et al. 2008b, *A&A*, 482, 499
- D’Ammando, F., Vercellone, S., Tavani, M., et al., 2009, *ATel*, 1957
- Dermer, C. D., Schlickeiser, R., Mastichiadis, A. 1992, *A&A*, 256, L27
- Donato, D., Ghisellini, G., Tagliaferri, G., Fossati, G. 2001, *A&A*, 375, 739
- Fabian, A. C. 1999, *MNRAS*, 308, L39
- Feroci, M., et al. 2007, *Nucl. Instr. Meth. Phys. Res. A*, 581, 728
- Gambill, J. K., Sambruna, R. M., Chartas, G., et al. 2003, *A&A*, 401, 505
- Gehrels, N., Chincarini, G., Giommi, P., et al. 2004, *ApJ*, 611, 1005
- Ghisellini, G., Maraschi, L., Tavecchio, F. 2009, *MNRAS*, 396, L105
- Gierlinski, M., Done, C. 2004, *MNRAS*, 349, L7
- Giuliani, A., et al. 2004, *Mem. Soc. Astron. Italiana Suppl.*, 5, 135
- Giuliani, A., et al. 2006, *Nucl. Instr. Meth. Phys. Res. A*, 568, 692
- Grandi, P., and Palumbo, G. 2004, *Science*, 306, 998
- Jorstad, S. G., Marscher, A. P., Lister, M. L., et al. 2005, *AJ*, 130, 1418
- Hartman, R. C., Bertsch, D. L., Fichtel, C. E., et al. 1992, *NASCP*, 3137, 116
- Hartman, R. C., Bertsch, D. L., Bloom, S. D., et al. 1999, *ApJS*, 123, 79
- Kalberla, P. M. W., Button, W. B., Hartmann, D., et al. 2005, *A&A*, 440, 775
- Kataoka, J., Mattox, J. R., Quinn, J., et al. 1999, *ApJ*, 514, 138
- Kataoka, J., Madejski, G., Sikora, M., et al. 2008, *ApJ*, 672, 787
- Labanti, C., Marisaldi, M., Fuschino, F., et al. 2009, *Nucl. Instr. Meth. Phys. Res. A*, 598, 470
- Laor, 1990, *MNRAS*, 246, L369 5
- Lawson, A. J., & Turner, M. J. L. 1997, *MNRAS*, 288, 920
- Lister, M. L., Homan, D. C., Kadler, M., et al. 2009, *ApJ*, 696, L22
- Malkan, M. A., & Moore, R. L. 1986, *ApJ*, 300, 216
- Maraschi, L., Ghisellini, G., Celotti, A. 1992, *ApJ*, 397, L5
- Marscher, A. P., Gear, W. K. 1985, *ApJ*, 298, 114
- Massaro, F., Tramacere, A., Cavaliere, A., et al. 2008, *A&A*, 478, 395
- Mattox, J. R. 1993, *ApJ*, 410, 609
- Mattox, J. R., Bertsch, D. L., Chiang, J., et al. 1996, *ApJ*, 461, 396
- Neugebauer, G., Oke, J. B., Becklin, E. E., et al. 1979, *ApJ*, 230, 79
- Nieppola, E., Valtoja, E., Tornikoski, M., et al. 2008, *A&A*, 488, 867
- Perotti, F., Fiorini, M., Incorvaia, S., et al. 2006, *Nucl. Instr. Meth. Phys. Res. A*, 556, 228
- Pian, E., & Treves, A. 1993, *ApJ*, 416, 130
- Pian, E., et al. 1999, *ApJ*, 521, 112
- Poole, T. S., Breeveld, A. A., Page, M. J., et al. 2008, *MNRAS*, 383, 627
- Prest, M., Barbiellini, G., Bordignon, G., et al. 2003, *Nucl. Instr. Meth. Phys. Res. A*, 501, 280
- Pucella, G., Vittorini, V., D’Ammando, F., et al. 2008, *A&A*, 491, L21
- Pucella, G., D’Ammando, F., Tavani, M., et al., 2009, *ATel*, 1968
- Raiteri, C. M., Villata, M., Lanteri, L., et al. 1998, *A&AS*, 130, 495
- Raiteri, C. M., Villata, M., Larionov, V. M., et al. 2007, *A&A*, 473, 819
- Raiteri, C. M., Villata, M., Larionov, V. M., et al. 2008, *A&A*, 491, 755
- Roming, P. W. A., Kennedy, T. E., Mason, K. O., et al. 2005, *Space Science Reviews*, 120, 95
- Sambruna, R. M., Barr, P., Giommi, P., et al. 1994, *ApJS*, 95, 371
- Sambruna, R. M., Tavecchio, F., Ghisellini, G., et al. 2007, *ApJS*, 669, 884
- Siebert, J., Brinkmann, W., Drinkwater, M. J., et al. 1998, *MNRAS*, 301, 261
- Sikora, M., Begelman, M. C., Rees, M. J. 1994, *ApJ*, 421, 153
- Singh, K. P., Rao, A. R., & Vahia, M. N. 1990, *ApJ*, 365, 455
- Singh, K. P., Shrader, C. R., & George, I. M. 1997, *ApJ*, 491, 515
- Smith, P. S., Elston, R., Berriman, R. G. 1988, *ApJ*, 326, L39
- Tanner, A. M., Bechtold, J., Walker, C. E., et al. 1996, *AJ*, 112, 62
- Tavani, M., Barbiellini, G., et al. 2008a, *Nucl. Instr. Meth. Phys. Res. A*, 588, 52
- Tavani, M., Barbiellini, G., et al. 2008b, *A&A*, in press
- Tavecchio, F., Maraschi, L., Ghisellini, G. et al. 2000, *ApJ*, 543, 535
- Tavecchio, F., Maraschi, L., Ghisellini, G. et al. 2007, *ApJ*, 665, 980
- Tavecchio, F., Ghisellini, G. 2008, *MNRAS*, 386, 945 980
- Tramacere, A., Massaro, F., Cavaliere, A. 2007, *A&A*, 463, 521
- Tramacere, A., 2008, *ATel*, 1743
- Türlér, M., et al. 2006, *A&A*, 451, L1
- Ulrich, M., Maraschi, L., Megan, C. M. 1997, *ARA&A*, 35, 445
- Urry, C. M., & Padovani, P. 1995, *Publication of the Astronomical Society of the Pacific. J Phys.*, 107, 803
- Vercellone, S., Chen, A. W., Giuliani, A., et al. 2008, *ApJ*, 676, L13
- Vercellone, S., D’Ammando, F., Pucella, G., et al. 2009, *ATel*, 1976
- Villata, M., Raiteri, C. M., Aller, M. F., et al. 2007, *A&A*, 464, L5
- Villata, M., Raiteri, C. M., Larionov, V. M., et al. 2008, *A&A*, 481, L79
- Wardle, J. F. C., Homan, D. C., Cheung, C. C., et al. 2005, *ASPC*, 340, 67
- Wills, B. J., Netzer, H., Wills, D. 1985, *ApJ*, 288, 94
- Woo, J., & Urry, C. M. 2002, *ApJ*, 579, 530

<sup>1</sup> INAF/IASF–Roma, Via Fosso del Cavaliere 100, I-00133 Roma, Italy

<sup>2</sup> Dip. di Fisica, Univ. di Roma “Tor Vergata”, Via della Ricerca Scientifica 1, I-00133 Roma, Italy

<sup>3</sup> INAF, Oss. Astronomico di Torino, Via Osservatorio 20, I-10025 Pino Torinese (Torino), Italy

<sup>4</sup> CIFS–Torino, Viale Settimio Severo 3, I-10133 Torino, Italy

<sup>5</sup> INAF, Istituto di Astrofisica Spaziale e Fisica Cosmica, Via U. La Malfa 153, I-90146 Palermo, Italy

<sup>6</sup> Dip. di Fisica and INFN Trieste, Via Valerio 2, I-34127 Trieste, Italy

<sup>7</sup> INFN–Pavia, Via Bassi 6, I-27100 Pavia, Italy

<sup>8</sup> Dip. di Fisica Nucleare e Teorica, Univ. di Pavia, Via Bassi 6, I-27100 Pavia, Italy

<sup>9</sup> INAF/IASF–Bologna, Via Gobetti 101, I-40129 Bologna, Italy

<sup>10</sup> INAF/IASF–Milano, Via E. Bassini 15, I-20133 Milano, Italy

<sup>11</sup> Dip. di Fisica Generale dell’Università, Via P. Giuria 1, I-10125 Torino, Italy

<sup>12</sup> ENEA–Bologna, Via dei Martiri di Monte Sole 4, I-40129 Bologna, Italy

<sup>13</sup> INFN–Roma “La Sapienza”, Piazzale A. Moro 2, I-00185 Roma, Italy

<sup>14</sup> INFN–Roma “Tor Vergata”, Via della Ricerca Scientifica 1, I-00133 Roma, Italy

<sup>15</sup> INAF–Oss. Astronomico di Cagliari, loc. Poggio dei Pini, strada 54, I-09012 Capoterra (CA), Italy

<sup>16</sup> Dip. di Fisica, Univ. dell’Insubria, Via Valleggio 11, I-22100 Como, Italy

<sup>17</sup> ENEA–Roma, Via E. Fermi 45, I-00044 Frascati (Roma), Italy

<sup>18</sup> Instituto de Astrofísica de Andalucía, CSIC, Apartado 3004, 18080 Granada, Spain

<sup>19</sup> Department of Astronomy, University of Michigan, Ann Arbor, MI 48109, USA

<sup>20</sup> Pulkovo Observatory, Russian Academy of Sciences, 196140, St.-Petersburg, Russia

<sup>21</sup> MPIfr, D-53121 Bonn, Germany

<sup>22</sup> Instituto de Astronomía, Universidad Nacional Autónoma de México, México, D. F. México

<sup>23</sup> Tuorla Observatory, Department of Physics and Astronomy, University of Turku, Väisäläntie 20, 21500 Piikkiö, Finland

<sup>24</sup> Astron. Inst., St.-Petersburg State Univ., 198504 St.-Petersburg, Russia

<sup>25</sup> INAF–Osservatorio Astrofisico di Catania, Via S. Sofia 78, I-95123 Catania, Italy

<sup>26</sup> Institute of Astronomy, National Central University, Taiwan

<sup>27</sup> Lulin Observatory, Institute of Astronomy, National Central University, Taiwan

<sup>28</sup> INAF, Osservatorio Astronomico di Roma, Via di Frascati 33, I-00040, Monte Porzio Catone, Italy

<sup>29</sup> INAF, Osservatorio Astronomico di Collurania, Via Mentore Maggini, I-64100 Teramo, Italy

<sup>30</sup> Harvard-Smithsonian Center for Astrophysics, Cambridge, Garden st. 60, MA 02138, USA

<sup>31</sup> Institute for Astrophysical Research, Boston University, 725 Commonwealth Avenue, Boston, MA 02215, USA

<sup>32</sup> ZAH, Landessternwarte Heidelberg, Königstuhl, D-69117 Heidelberg, Germany

<sup>33</sup> Instituto de Astronomia, Universidad Nacional Autonoma de Mexico, 2280 Ensenada, B.C. Mexico

<sup>34</sup> Abastumani Observatory, 383762 Abastumani, Georgia

<sup>35</sup> INAF–IRA, contrada Renna Bassa, I-96017 Noto (SR), Italy

<sup>36</sup> Department of Physics and Astronomy, University of Southampton S017 1BJ, UK

<sup>37</sup> INAOE, Apdo. Postal 51 y 216, 72000 Tonantzintla, Puebla, Mexico

<sup>38</sup> Lowell Observatory, Flagstaff, AZ 86001, USA

<sup>39</sup> ASI–ASDC, Via G. Galilei, I-00044 Frascati (Roma), Italy

<sup>40</sup> ASI, Viale Liegi 26, I-00198 Roma, Italy